Analyst

Dynamic Article Links

Cite this: *Analyst*, 2012, **137**, 3255

www.rsc.org/analyst

PAPER

The effect of anticancer drugs on seven cell lines monitored by FTIR spectroscopy

Allison Derenne, Magali Verdonck and Erik Goormaghtigh*

Received 25th January 2012, Accepted 3rd May 2012
DOI: 10.1039/c2an35116a

Systemic approaches such as metabolomics are increasingly needed to improve the development of novel drugs. In this paper, we suggest a new strategy based on infrared spectroscopy which probes the global chemical composition of a sample. Seven cell lines from three tumour types were investigated and exposed to four classical anticancer drugs belonging to two classes characterized by a unique mechanism. First, each cell line was considered separately and a hierarchical clustering was built for the seven cell lines. Spectra clustered according to the drug mechanism of action for all the cell lines tested. Second, the similarities among drug mechanism spectral fingerprints were investigated for all the cell lines simultaneously. Difference spectra (the mean spectrum of the corresponding untreated cell line was subtracted) were computed so that the particular contribution of every cell line was eliminated and only the drug-induced differences could be compared. The hierarchical clustering shows a clear tendency to distinguish the two modes of action, revealing a very similar type of response to molecules with a similar mechanism. High throughput systems with 96-well plates are now available and a well established bioassay could be developed in order to provide an objective classifier for potential anticancer drugs.

Introduction

In recent years, the development of novel drugs has become increasingly difficult, expensive and time-consuming. It is estimated that more than 800 million USD and an average of 14.2 years are required for a novel drug application approval.[1] The decreasing number of novel drugs every year leads to growing interest in developing new methodologies for the detection of active compounds. Progressively, more systemic approaches are applied in order to obtain a global insight into the biological and physiological processes. One of the promising tools for new strategies is the use of metabolomics.[2,3] Metabolomics is the study of global metabolite profiles in a system (cells, tissue or organism) under a given set of conditions. Metabolites are the results of the interaction of the system's genome with its environment and are not only the end product of gene expression but are also part of the regulatory system in an integrated manner.[2]

In this context, it could be interesting to develop a strategy based on infrared spectroscopy. This technique monitors the global chemical composition of a sample. A spectrum of cells is a superimposition of spectra of all cell constituents.[4] Furthermore, the IR spectra account not only for the chemical nature of cell molecules but also for their conformations and are, in particular, very sensitive to protein secondary structure.[5] This sum of information has already been used for various applications in a context of systemic approach. Thirty years ago, it was demonstrated that IR spectra of bacteria allow a classification as accurate as the one built with current phylogeny techniques. The precise fingerprints obtained with IR spectroscopy lead also to the identification of new species.[6,7] Nowadays, it is even possible to distinguish wild-type toxic strains and the probiotic strains of the same species (*Bacillus cereus*).[8] This approach was also used to study eukaryotic cells and in particular cancerous cells. First of all, changes between normal and cancerous cells were observed for various types of cancers by FTIR spectroscopy. Thereby, it was possible to identify abnormal cells even if no morphological symptom was visible. IR spectroscopy became a powerful tool for cell line identification, biodiagnostics and prognostics.[9,10] *In vitro*, closely related cancer cells could be distinguished. For instance, the FTIR spectra of various human glioma cell lines were shown to be strongly correlated with their aggressiveness *in vivo*.[11]

As the previous examples underline, infrared spectroscopy yields a precise image of all the chemical bonds present in the sample and offers the opportunity to observe very quickly all metabolic modifications induced by a treatment. Recent publications have evidenced that different drug actions yield each a unique fingerprint characteristic of the "mode of action" of the agent under investigation. In turn drug-induced metabolic disorders are amenable to classification similar to the ways by which bacteria gender, species, and strains can be classified.

Center for Structural Biology and Bioinformatics, Laboratory for the Structure and Function of Biological Membranes, Campus Plaine CP206/02, Université Libre de Bruxelles, Bld du Triomphe 2, CP206/2, B1050 Brussels, Belgium. E-mail: egoor@ulb.ac.be; Fax: +32-2-650-53-82; Tel: +32-2-650-53-86

Anticancer cardiotonic steroids with closely related structures but distinct effects on a prostate cancer cell line (PC-3) could be distinguished by FTIR spectroscopy.[12] Draux *et al.* also demonstrated that spectral modifications induced by gemcitabine on non-small lung cancer Calu-1 could be associated with drug concentrations and exposure times.[13] A study of Flower *et al.* showed that A2780 ovarian cancerous cells when treated with a range of 5 different drugs known to operate by different mechanisms can be distinguished from each other and from untreated cells using synchrotron radiation infrared microspectroscopy.[14] Finally, in a previous paper, we used FTIR spectroscopy to test the action of 7 anticancer drugs belonging to 3 different classes on human prostate cancer PC-3 cells. Difference spectra between treated and untreated cells and Student's *t*-test provided a spectral signature of the effect of each compound on PC-3 cells. Interestingly, drugs known to induce similar types of metabolic disturbances appear to cluster when spectrum shapes are analyzed.[15] Yet, these studies were carried out on a single cell line. The present work addresses two main questions. First, we will examine if spectral clustering by mechanism of action is specific to PC-3 cells or can be extended to other cell lines. Second, we will investigate whether the spectral fingerprint of one "mode of action" is similar for all the cell lines. To analyse these two issues, 7 cell lines from 3 tumour types are considered and exposed to 4 classical anticancer drugs belonging to two classes characterized by a unique mechanism. The first class, the antimicrotubules (paclitaxel and vincristine), affects in particular microtubules and blocks formation or dissociation of spindle apparatus which separates the chromosomes into the daughter cells during cell division.[16–18] The second class includes doxorubicin and daunorubicin; they inhibit class II topoisomerases progression, preventing the DNA double helix from being resealed and therefore stopping cell division.[19,20]

Two cell lines derive from lung carcinoma (A549 and A427); two other cell lines come from prostate carcinoma (PC-3 and DU145). The last three (T98G, U373 and Hs683) are glioblastoma.

Materials and methods

1. Cell culture and treatment

The human prostate cancer PC-3 (ACC 465) and lung cancer A549 (ACC 107) cell lines were obtained from the Deutsche Sammlung von Mikroorganismen und Zellkulturen (DSMZ, Braunschweig, Germany).

The human T98G (CRL-1690) and Hs683 (HTB-138) glioblastoma cell lines, the human prostate cancer DU-145 (HTB-81) and the human lung cancer A427 (HTB-53) cell lines were obtained from the American Type Culture Collection (ATCC, Manassas, VA). The human U373 (89081403) glioblastoma cell line was obtained from the ECACC collection (Sigma Aldrich).

All cell lines were maintained according to the supplier's instructions. They were incubated at 37 °C in sealed (airtight) Falcon plastic dishes (Cellstar, Greiner Bio-one, Wemmel, Belgium) in a humidified atmosphere of 5% CO_2. The cells were kept in exponential growth in RPMI medium supplemented with 10% fetal bovine serum (FBS), 2% penicillin–streptomycin (an antibiotic solution). Cell culture medium, FBS and antibiotics were purchased from Lonza (Verviers, Belgium). Our cultures were frequently tested for mycoplasma infections using PlasmoTest from InvivoGen (Toulouse, France).

2. Determination of IC_{50} growth inhibitory concentrations

Drug concentrations used throughout this work relate to the IC_{50} concentrations that are defined as the drug concentration required for decreasing the global growth levels of a given cell population by 50% after 72 h. IC_{50} concentrations are calculated by means of the MTT (3-[4,5-dimethylthiazol-2yl]-diphenyltetrazolium bromide, Sigma, Bornem, Belgium) colorimetric assay as detailed elsewhere[21] and briefly summarized as follows. All cell lines were incubated for 24 h in 96-microwell plates to ensure adequate cell adhesion before treatment. After this initial 24 h step, the 4 anticancer drugs were assayed for 72 h from 0.1 nM up to 1 μM for antimicrotubules and from 1 nM up to 10 μM in the case of topoisomerase inhibitors. The cell population growth in control and treated conditions is determined according to the capability of living cells to reduce the MTT yellow product into the formazan blue product by a reaction occurring in the mitochondria.[21,22] Thus, the number of living cells after 72 h of culture in the presence (or absence: control) of the various compounds is directly proportional to the intensity of the blue staining, which is quantitatively measured by spectrophotometry – in our case using a Biorad Model 680XR (Biorad, Nazareth, Belgium) at a 570 nm wavelength (with a reference of 630 nm). Each experiment was carried out in sextuplicate.

3. FTIR spectroscopy

For the FTIR spectroscopy, cells were exposed to the four anticancer drugs at their respective IC_{50} concentrations (obtained by means of the MTT colorimetric assay) for 24 h. Cells were then detached from their culture support by means of a five minute treatment with 1 ml of trypsin (0.5 g l^{-1})/EDTA 0.2 g l^{-1} buffer (Lonza, Verviers, Belgium). The reaction was stopped by adding 1 ml of culture medium. The cells were pelleted by a 2 minute centrifugation (300*g*), and washed three times in isotonic solution (NaCl, 0.9%) to ensure complete removal of trypsin and culture medium; they were then resuspended in around 10 μl of the NaCl solution.

All measurements were carried out on a Bruker Equinox 55 FT-IR spectrometer (Bruker, Karlsruhe, Germany) equipped with a liquid N2-refrigerated mercury cadmium Telluride detector. All spectra were recorded by attenuated total reflection (for a review, see ref. 23). A diamond internal reflection element was used on a Golden Gate Micro-ATR from Specac (Orpington, UK). The angle of incidence was 45 degrees. A 0.5 μl amount of the resuspended cell was deposited on the diamond crystal (about 3×10^4 cells per smear). The sample was quickly evaporated in N_2 flux to obtain a homogeneous film of whole cells, as ascertained by microscope examination. The FT-IR measurements were recorded between 4000 and 800 cm^{-1}. Each spectrum was obtained by averaging 256 scans recorded at a resolution of 2 cm^{-1}. A minimum of two independent cultures were grown for each condition and three samples were taken from each culture for infrared measurement. Experiments were at least reproduced twice and a minimum of twelve spectra per condition were generated.

4. Data analyses

All the spectra were preprocessed as follows. The water vapour contribution was subtracted as described previously[24,25] with 1956–1935 cm^{-1} as the reference peak. The spectra were then baseline-corrected over the whole spectrum and normalized for equal area between 1582 and 1492 cm^{-1} (amide II peak). In principle, normalization can be performed on any part of the spectrum as relative intensities are used for comparison. By using the amide II region, which mostly, but not only, represents protein contribution, we avoid including the amide I region which is usually disturbed by small variations in the water content of the sample. The spectra were also smoothed at a final resolution of 4 cm^{-1} by apodization of their Fourier transform by a Gaussian line. Finally, the signal/noise (S/N) ratio was systematically checked on every spectrum. It was required to be greater than 450 when noise was defined as the standard deviation in the 2000–1900 cm^{-1} region of the spectrum and the signal is the maximum of the curve between 1750 and 1480 cm^{-1} after a baseline passing through these two points had been subtracted.

Normality of the distribution of the absorbances was checked for each group at every wavenumber by a Kolmogorov–Smirnov test by comparison with a standard normal distribution, with a confidence level $\alpha = 0.5\%$ (not shown). The results demonstrated the normality of absorbance distributions.

4.1. Difference spectra and Student's *t*-test. In order to evidence spectral variations induced by each of the molecules, the mean spectra of untreated cells (controls) were subtracted from the mean spectra of treated cells for all conditions. We thus obtained the "difference spectra", which represent the actual metabolic modifications caused by each compound with respect to each cell line. All difference spectra were calculated with fully preprocessed spectra (baseline corrected and normalized). Student's *t*-test was computed at every wavenumber and allowed a statistical comparison between the spectra of cells incubated in the presence of a drug and the control cell spectra. Wavenumbers where a significant difference occurs (with a significance $\alpha = 0.5\%$) are indicated by thicker lines.

4.2. Hierarchical cluster analysis. Hierarchical classification builds groups with most similar data using Ward's algorithm. Ward's linkage used here is a method allowing hierarchical clustering of n groups with minimum loss of information. It is based on the similarity of group members with respect to many variables.[26,27] The Euclidian distance between all the spectra is calculated and the grouping is based on the error sum of square criterion (ESS). At each step of the grouping procedure, each possible union is considered and the two items with the lower ESS are grouped. The process is repeated until the number of groups is reduced from n to 1.[26,27]

Correction of the spectra, Kolmogorov–Smirnov and Student's *t*-tests and hierarchical classification were carried out by Kinetics, a custom made program, running under Matlab 7.1 (Matlab, Mathworks Inc.).

Results

In a first step, the concentration inhibiting 50% of the cell growth after 72 h, called here IC_{50}, was evaluated for each drug on the seven cell lines. This is a reference commonly used in pharmaceutical studies to compare the effect of various products. As this value can strongly depend on cell lines and culture conditions, it was important to determine it on each cell line for our particular culture settings. These IC_{50} values are presented in Table 1. The data show that indeed the IC_{50} of a drug strongly varied from cell line to cell line. Antimicrotubule agents displayed IC_{50} that range for paclitaxel between 0.75 and 9.3 nM and for vincristine between 4.1 and 55 nM. However, the range of concentration for topoisomerase inhibitors was much larger, between 32.3 and 1660 nM.

For all the infrared experiments, cells were grown to subconfluence *ca.* 80% of confluence as defined elsewhere[28] and exposed to the drugs for 24 h (*ca.* 1 generation time). Selecting 24 hours is a choice that allows the recording of strong and specific spectral variations with minimal generic damage to the cells (apoptosis, necrosis, …). Untreated cells from the same cell line were always grown in parallel as a control. For each experiment, a minimum of 6 spectra originating from 2 culture flasks were recorded for all conditions. All experiments were repeated at least twice.

Fig. 1 displays the mean spectra (solid lines) and standard deviations calculated at every 1 cm^{-1} (dotted lines) of cells incubated with the drug indicated in the right margin. These spectra are very similar at first glance with the standard deviation almost overlapping the spectra. Statistical analyses were applied, first in order to compare spectral modifications induced by the 4 drugs on each cell line and, second, to investigate the similarity of spectral changes induced by each drug on all the cell lines taken together.

1. Classification of drug mechanisms for each cell line

The wording drug "mechanism" or drug "mode of action" is used below to qualify drugs that target either class II topoisomerases (daunorubicin and doxorubicin) or tubulin (paclitaxel and vincristine). The question addressed here was to establish whether for each cell line drug-induced spectral modifications are primarily related to drug mechanism. Difference spectra and Student's *t*-test were calculated (see Materials and methods) as illustrated in Fig. 2A for the A427 cell line. The shape of difference spectra evidences spectral variations representing metabolic perturbations induced by each molecule on this cell line. Thicker lines indicate wavenumbers significantly different as calculated by the Student's *t*-test with a significance of 0.5%. In Fig. 2A, it can be observed that spectral variations appear to be associated with the mode of action of the two groups of drugs used for A427 cells. Indeed, the shape of the difference spectra of topoisomerase inhibitors is analogous, *i.e.* positive and negative peaks are found at similar wavenumbers with comparable intensities. Similarities among antimicrotubules can also be noticed, for example, the peak around 1735 cm^{-1} and the region between 1500 and 1350 cm^{-1}. Furthermore, significantly different zones (indicated by thicker lines) also appear at similar wavenumbers for drugs characterized by a similar mode of action.

It can be noticed that radical changes in the lipid to protein ratio are clearly observed in Fig. 2A between topoisomerase inhibitors and antimicrotubules. An exact interpretation of this difference is beyond the scope of this publication. However, it can be underlined that the activation of lipid metabolism is an early event in carcinogenesis and a central hallmark of many

Table 1 IC_{50} of the 4 anticancer drugs on the seven cell lines used in this work. Concentration of drug reducing cell growth by 50% after 72 h (IC_{50}) were determined by the MTT procedure as described in "Methods"

IC_{50} (nM)		A427	A549	T98G	U373	Hs683	DU145	PC3
Topoisomerase inhibitors	Daunorubicin	451.7 ± 145	170.9 ± 21	629.6 ± 130	41 ± 0.4	170.3 ± 55	32.3 ± 8.2	375.4 ± 41
	Doxorubicin	677.7 ± 237	184.3 ± 161	1660.7 ± 962	78.5 ± 11.5	176.9 ± 76	75.1 ± 8	338.2 ± 105
Antimicrotubules	Paclitaxel	7.3 ± 2.7	6.2 ± 0.6	6.9 ± 1.6	6.5 ± 0.6	4.5 ± 0.07	0.75 ± 0.07	9.3 ± 2.8
	Vincristine	5.2 ± 2.8	47.1 ± 7.3	42.8 ± 10.4	4.1 ± 0.2	45.3 ± 2.2	55 ± 23	8.6 ± 1.2

cancers.[29] Moreover, when apoptosis is triggered, changes in the phosphatidylserine distribution between the inner and outer leaflet of the membrane can be rapidly observed.

The similarities in shape can be quantified using hierarchical classification. Fig. 2B shows the clustering obtained for the spectra displayed in Fig. 2A. The two major classes observed on the clustering correspond to the two types of mechanisms.

A similar analysis was applied to each cell line independently and similar observations were made. Fig. 3 displays the seven clusterings obtained. All these classifications were built considering wavenumbers between 1800 and 900 cm^{-1} and show 2 groups corresponding to the two modes of action. It must be noticed that this approach is unsupervised, which means that no *a priori* knowledge about the drug was required. Yet, spectra group spontaneously according to the mode of action of the molecules.

2. Comparison between cell lines

The question addressed here was to determine to which extent the spectral signatures of one mode of action, as defined above, are similar for all the cell lines. In order to compare different cell lines which already have significantly different spectra before any exposure to a drug, the mean of spectra of untreated cells was always subtracted. In turn, the particular contribution of the cell line was eliminated and only the drug-induced differences were compared. Fig. 4A displays the difference spectra for all the cell lines exposed to topoisomerase inhibitors and Fig. 4B shows those for antimicrotubule agents. It can be noticed that the difference spectra appear more related to drug mode of action between 1300 and 900 cm^{-1} than elsewhere. In this zone, the absorption is mainly due to carbohydrates and phosphates, especially phosphate groups associated with nucleic acids (DNA

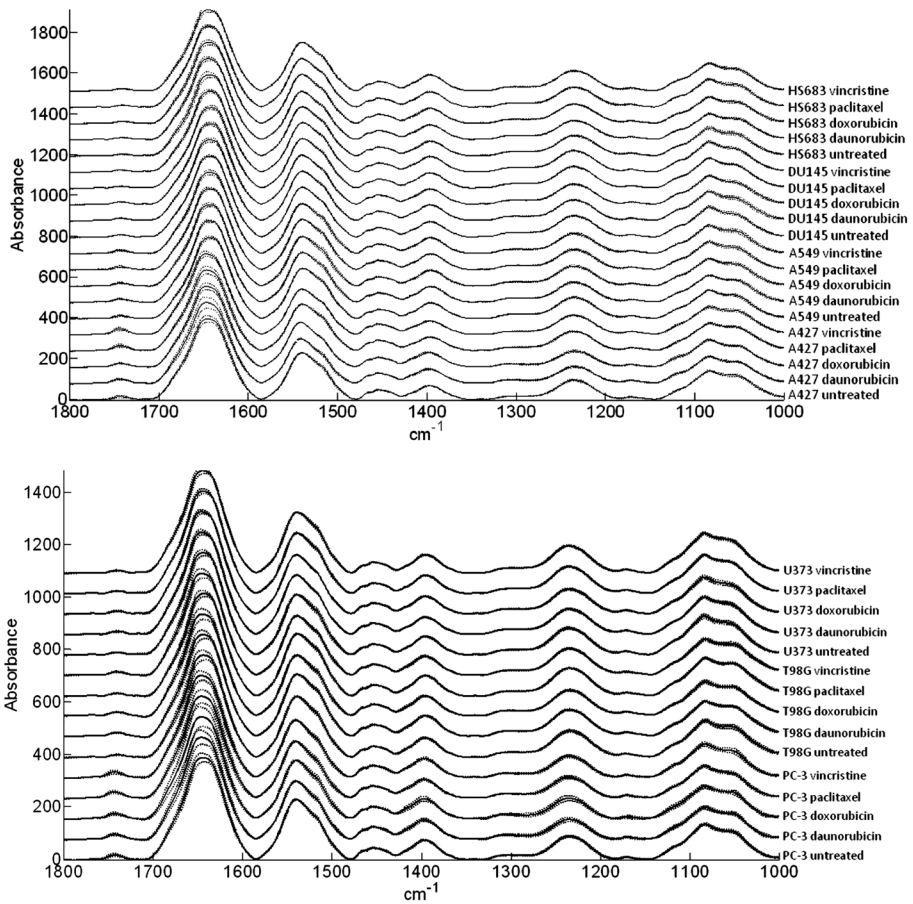

Fig. 1 Mean infrared spectra (solid lines) ± standard deviation (dotted lines) of all conditions; cell lines and drugs are indicated in the right margin. At least 10 spectra were recorded for each mean spectrum presented here. Spectra were processed as described in Materials and methods and have been normalized to the same arbitrary area between 1582 and 1492 cm^{-1}. Spectra have been offset for better readability.

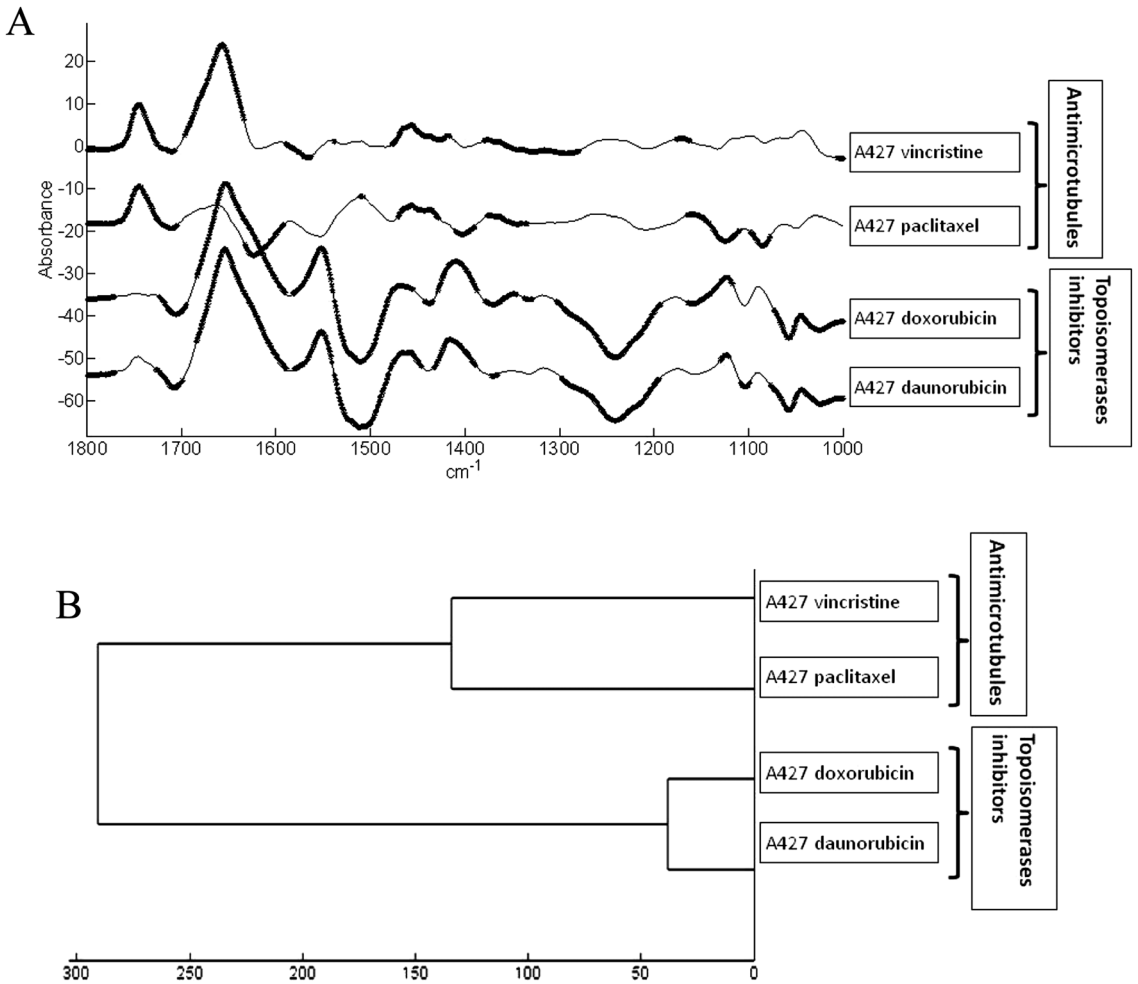

Fig. 2 (A) Differences between the mean spectra obtained for A427 cells exposed to a drug (as indicated in the right margin) and control cells. Spectra have been normalized to the same area under 1582 and 1492 cm^{-1} prior to subtraction. Spectra have been offset for a better readability. A Student's *t*-test was computed at every wavenumber with a significance level of $\alpha = 0.5\%$. Each marked wavenumber (thicker lines) indicates a statistically significant difference between the means. (B) Hierarchical classification of the difference spectra presented in (A) considering the spectral region between 1800 and 900 cm^{-1}.

and RNA). The peaks appearing at 1241 and 1085 cm^{-1} (ref. 30) are characteristic of the asymmetric and symmetric phosphodiester vibrations of nucleic acids.[31,32]

The similarities among these spectra appear more clearly on a dendrogram built using hierarchical classification using the region between 1300 and 900 cm^{-1}. The clustering is presented in Fig. 5 and shows a clear tendency to distinguish the molecules according to the two modes of action when all cell lines are taken together. The primary separation in two groups (line A, Fig. 5) largely corresponds to drug mechanisms. On 28 spectra, 4 would be misclassified according to the "mode of action". A549 and PC-3 exposed to antimicrotubules indeed cluster with topoisomerase inhibitors.

Line B evidences, within the antimicrotubules group, that T98G spectra cluster separately from the others, and separates 3 groups inside the topoisomerase inhibitor cluster which will be discussed later. The final node (thicker lines, Fig. 5) systematically classifies together cell lines exposed to either doxorubicin and daunorubicin or paclitaxel and vincristine (except for A427 and U373 exposed to antimicrotubules).

Discussion

FTIR spectroscopy was recently demonstrated to be a useful tool to obtain a unique fingerprint of anticancer drugs such as platinum derivatives[33] or cardiotonic steroids.[12,28,34] Furthermore, it was demonstrated that FTIR could classify 7 anticancer drugs in 3 groups corresponding to the 3 mechanisms of action of the drug tested.[15] Yet, whether this would apply to other cell lines was not addressed. In the present paper, the effect of 4 drugs, 2 antimicrotubules and 2 topoisomerase inhibitors was evaluated on seven cell lines.

Any comparison between drugs and cell lines requires a normalisation. As it is clearly illustrated in Table 1, the sensitivity of cancer cells strongly depends on the cell line and the IC_{50}, the concentration inhibiting 50% of the cell growth after 72 h of incubation with the drugs, provides such a normalisation. At this drug concentration, cells are still living but the growth rate is reduced. Furthermore, if dead cells were present, they floated in the medium and were eliminated by washing prior to harvesting the cells.

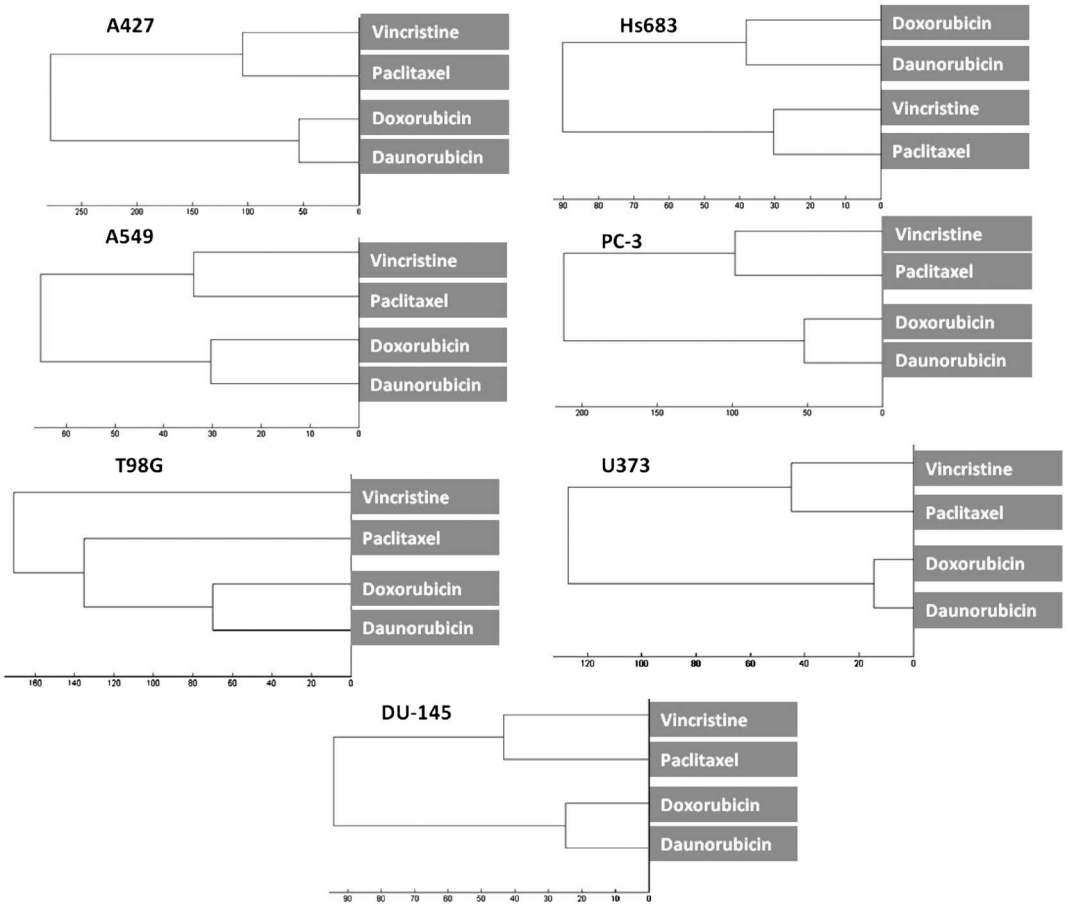

Fig. 3 Hierarchical classification of all the cell lines exposed to 4 drugs as indicated on the figure. Difference spectra similar to the ones shown in Fig. 2A were computed for all the cell lines and submitted to hierarchical clustering on the 1800–900 cm^{-1} region as described in Fig. 2B.

The results obtained here on 7 cell lines confirm that for each cell line hierarchical clustering allows a separation according to the drug mode of action. Interestingly, for all the cell lines except Hs683, we observe in Fig. 3 a shorter distance (horizontal axis) between topoisomerase inhibitors compared to anti-microtubules. A potential rationale is that the former both inhibit type II topoisomerases while the latter target two distinct processes, respectively microtubule polymerisation and depolymerisation. Even though microtubules are targeted in both cases, they either do not polymerize or do not depolymerise, resulting in a significantly different situation for the cells. Yet, in both cases mitosis is blocked and the global chemical content probed by FTIR spectroscopy is similarly affected. This difference might also explain the particular shape of the clustering for the cell line T98G as shown in Fig. 2.

Overall, difference spectra and the Student's *t*-test provide a spectral signature of the effect of a compound on each cell line which suggests that spectral modifications can be associated with a particular drug mechanism for the 7 cell lines. As high throughput methods are now available to record FTIR spectra of cells, more experiments could be carried out to create a large database of drug "mode of action" signatures.

The molecular origin of the spectral differences is difficult to establish considering the large variety of molecules in the cells. A contribution of the drug molecules themselves can be ruled out as demonstrated in the Appendix. Spectra of each drug at a 10^{-4} M concentration were recorded. At this concentration drug spectral contribution is not observable, only traces of water vapour are apparent (Fig. 6, Appendix). Yet this concentration is 100 to 1000 times higher for topoisomerase inhibitors and at least 10 000 times higher for antimicrotubules than the one used for treating the cells. In order to provide a second evidence for the absence of interference from drug spectra, the actual spectra of drug molecules (which required much higher concentration) have been compared with the corresponding difference spectra for two cell lines (Fig. 7 in the Appendix). These spectra display very few similarities strongly suggesting that the drugs themselves do not contribute to the spectral variations.

A contribution from cell molecules conformational changes could also contribute to the difference spectra. Yet, as far as the conformation of macromolecules is concerned (protein, DNA, …), the spectral signatures recorded are not typical of conformational changes (*e.g.* Fig. 4). For instance, a conformational change in a protein would be reflected by a typical sigmoid feature in the amide I region, indicating a relative change in the proportion of the various secondary structure types. Such sigmoid shapes are not observed.

If the difference spectra features are not due to the drugs themselves or to conformational changes, it may be hypothesized that they are related to changes in relative concentrations of

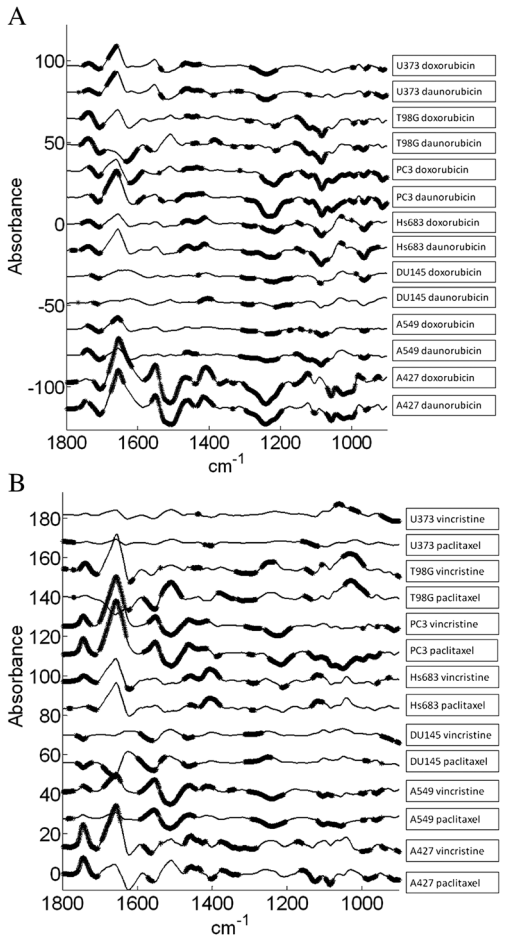

Fig. 4 (A) Differences between the mean spectra (see Fig. 2A for details) of cells exposed to topoisomerase inhibitors and the untreated counterparts of the same cell lines (as indicated in the right margin). (B) Same figure as (A) but cells are exposed to antimicrotubules. All the spectra are at the same scale and the magnitudes of the difference are real. A Student's *t*-test was computed at every wavenumber with a significance level of $\alpha = 0.5\%$. Each marked wavenumber (thicker lines) indicates a statistically significant difference between the means.

proteins, lipids, and DNA. It must be emphasized that after 24 hours of exposure, cells have undergone considerable changes involving a very large number of molecules. Besides, most spectral regions are affected:

- In Fig. 4, for both classes of drugs and many cell lines, significant changes appear around 1735 cm^{-1}. This band can be assigned to the ester C═O stretching of the phospholipids and is not significantly overlapped by contributions from DNA and proteins.[35,36] As mentioned previously, lipids are known to be involved in many biological pathways, in particular in tumorigenesis.

- Nearly all difference spectra (Fig. 4) exhibit significant differences between 1700 and 1300 cm^{-1}. In this region, the absorptions are primarily due to the proteins. Stretching of the carbonyl group from the peptide bond takes place around 1650 cm^{-1} (named amide I). This band is sensitive to the secondary structure of proteins. The deformation of the protein N–H bond (amide II) appears around 1550 cm^{-1}.[23] The bands between 1480 and 1300 cm^{-1} result from various amino acid side chains and fatty acids. Adding drugs in cell culture obviously triggers various metabolic pathways which caused changes in the total protein content.

- In Fig. 4, every difference spectra display significant variations between 1300 and 900 cm^{-1}. This zone is dominated by the absorption of carbohydrates and phosphates, especially phosphate groups associated with nucleic acids (DNA and RNA). As discussed later, the drugs used in this work are known to cause changes in nucleic acids.

Most interestingly, when difference spectra were compared for the seven cell lines used in this work, the first level of clustering appears to group spectra according to their mode of action, whatever the cell line, indicating that the spectral signature of the effect of molecules on most cell lines is largely independent of its particular phenotype. However, 4 spectra out of 28 were misclassified according to this criterion. PC-3 and A549 cells exposed to antimicrotubules stand in the wrong group indicating that in some cases the particular response of the cell line may dominate, underlying the heterogeneity of metabolic responses

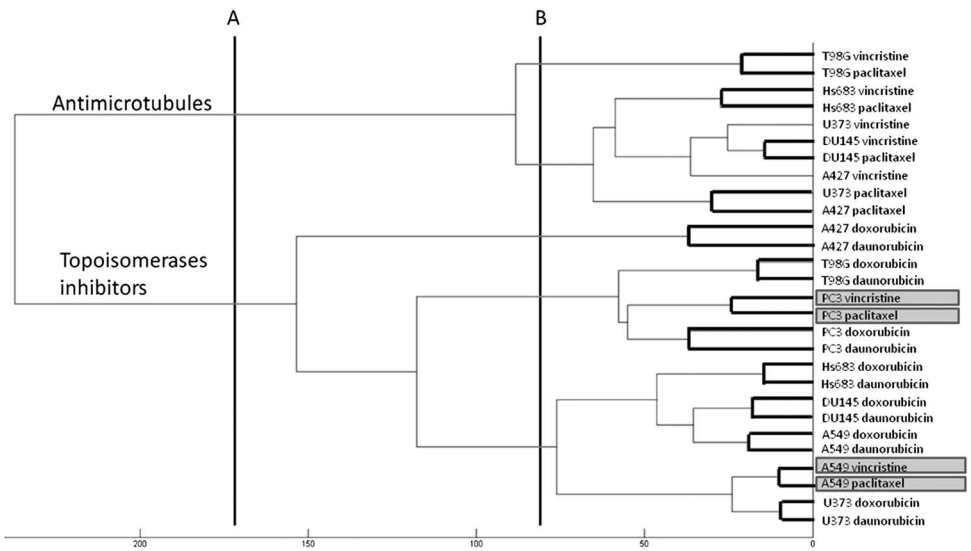

Fig. 5 Hierarchical classification of the spectra presented in Fig. 4 considering the spectral region between 1300 and 900 cm^{-1}.

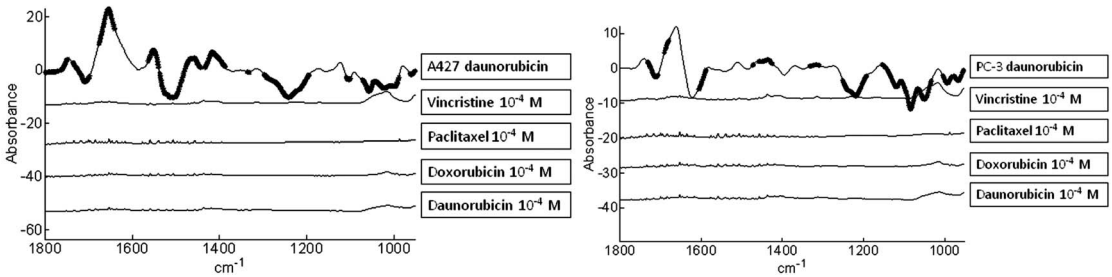

Fig. 6 Comparison between the difference spectra corresponding to A427 (left) and PC-3 (right) exposed to daunorubicin (top) and pure drug spectra. For pure drug spectra, 0.5 μl of 10^{-4} M drug was dried on the diamond ATR surface, *i.e.* a volume corresponding to the volume of the cell pellet used. As scaling of cell spectra used for computing the difference spectra (see Methods) results in a *ca.* 1000 fold intensity enhancement, the pure drug spectra were multiplied by 1000. Spectra were drawn at the same scale and are offset for better readability.

following exposition to a drug and the necessity of working on various cell lines. One potential explanation for this "misclassification" is a difference in the intensity of the response. It could be questioned whether the intensities of the difference spectra are responsible for the classification observed in Fig. 5. To answer this question, difference spectra of Fig. 4 were rescaled (vector normalisation between 3000 and 2800 cm^{-1} and between 1765 and 950 cm^{-1}). This correction was found to further degrade the classification, suggesting that the obtained classification is not related to difference in response intensities. In turn, it is likely that cell line specificities are responsible for the variability in the response to anticancer drugs.

When considering all the cell lines together, it appears that some cell lines display dramatically different behaviour with respect to the drugs. Table 1 reveals large differences, in particular for doxorubicin which displays an IC_{50} of 75 nM for DU145 and 1660 nM for T98G. It suggests that resistance mechanism might be involved. Indeed, several publications have demonstrated that T98G, for example, exhibits a constitutive multidrug resistance phenotype often associated with the expression of the human *mdr*-1 gene product, P-glycoprotein.[37,38] Multiresistant phenotypes could induce slightly different metabolic consequences when exposed to a drug. Line B in Fig. 5 reveals 3 groups that might be linked to the resistance phenotype: one for A427, one for T98G and PC-3, and one with all the other cell lines. Interestingly, PC-3, A427 and T98G present higher IC_{50} for topoisomerase inhibitor compounds (ranging between 338 and 1660 nM) while other cell lines (Hs683, U373 and A549) show lower IC_{50} (ranging between 32 and 184 nM) (see Table 1).

Two cell lines were considered as displaying an extreme and opposite behaviour with respect to apoptosis. The PC-3 cell line appeared as very sensitive to proapoptotic stimuli.[39] Therefore, after 24 hours of incubation, a biochemical signal leading to cellular death might dominate in comparison with the metabolic pathways specific to a treatment. The case of A549 is opposite, this cell line is considered most resistant to a series of cell death mechanisms including apoptosis.[40] A hypothesis to explain the misclassification of A549 could be that biochemical signals of these resistant mechanisms prevail against those induced by the treatment.

Grouping discussed in this work has been obtained by unsupervised statistical analyses. Yet, selection of the spectral range introduces some degree of supervision. It must be noted that clusters built for each cell line (Fig. 3) appear quite robust with respect to spectral range. Other spectral zones were tested: 1600–900 cm^{-1}, 1400–900 cm^{-1}, 1300–900 cm^{-1} and 1800–900 + 3000–2800 cm^{-1}. All the spectral ranges led to a separation between the 2 classes of molecules, similar to the one presented in Fig. 3. However, when comparing the seven cell lines together (Fig. 4), the region between 1800 and 900 cm^{-1} did not lead to any coherent classification. In order to evidence a common drug mechanism signature, we looked up for the spectral range that led to the best separation between the 2 classes. Therefore, we tested various spectral ranges and selected the 1300–900 cm^{-1} region. This region is dominated by DNA and RNA phosphate absorbance. This is not surprising considering the mechanism of these drugs. Antimicrotubules block cells in the mitosis phase. At this stage, cells contain 2 copies of DNA in comparison with cells in the G0/G1 phase (around 65% of untreated cells). When topoisomerases are inhibited, cells are blocked in the synthesis phase. There is therefore a major difference in DNA content when cells are exposed to the two types of drugs.

In this work, the term "mode of action" was used to describe the documented mechanism by which drugs decrease the cell growth rate. It was correlated, through the FTIR spectra, to the global modifications of cell chemical content upon exposure to a drug. This FTIR-derived observation does not necessarily imply any particular biochemical mechanism but was found to be useful for drug classification purposes. It has recently been reported[41] that Raman spectroscopy of cells exposed to cisplatin could pinpoint spectral changes that have their origin either in the biochemical interaction of the drug with the cell or its physiological response. In the present work significant changes that appear in IR spectra rather reflect the complex physiological consequences of the initial drug binding. After 24 hours (*ca.* one generation time), these metabolic consequences are already intense and potentially affect all types of molecules. It can indeed be observed that spectral regions dominated by lipid, protein and nucleic acid contributions are significantly modified. Furthermore, changes in cell shape (data not shown) clearly appear under the microscope after 24 h, revealing a global effect of the drug treatment. It was beyond the scope of the present paper to define how initial some of these spectral changes may be. It was also beyond the scope of the paper to provide a detailed analysis of the spectral changes and of the particularities that exists among cell lines, possibly with respect to their genetic

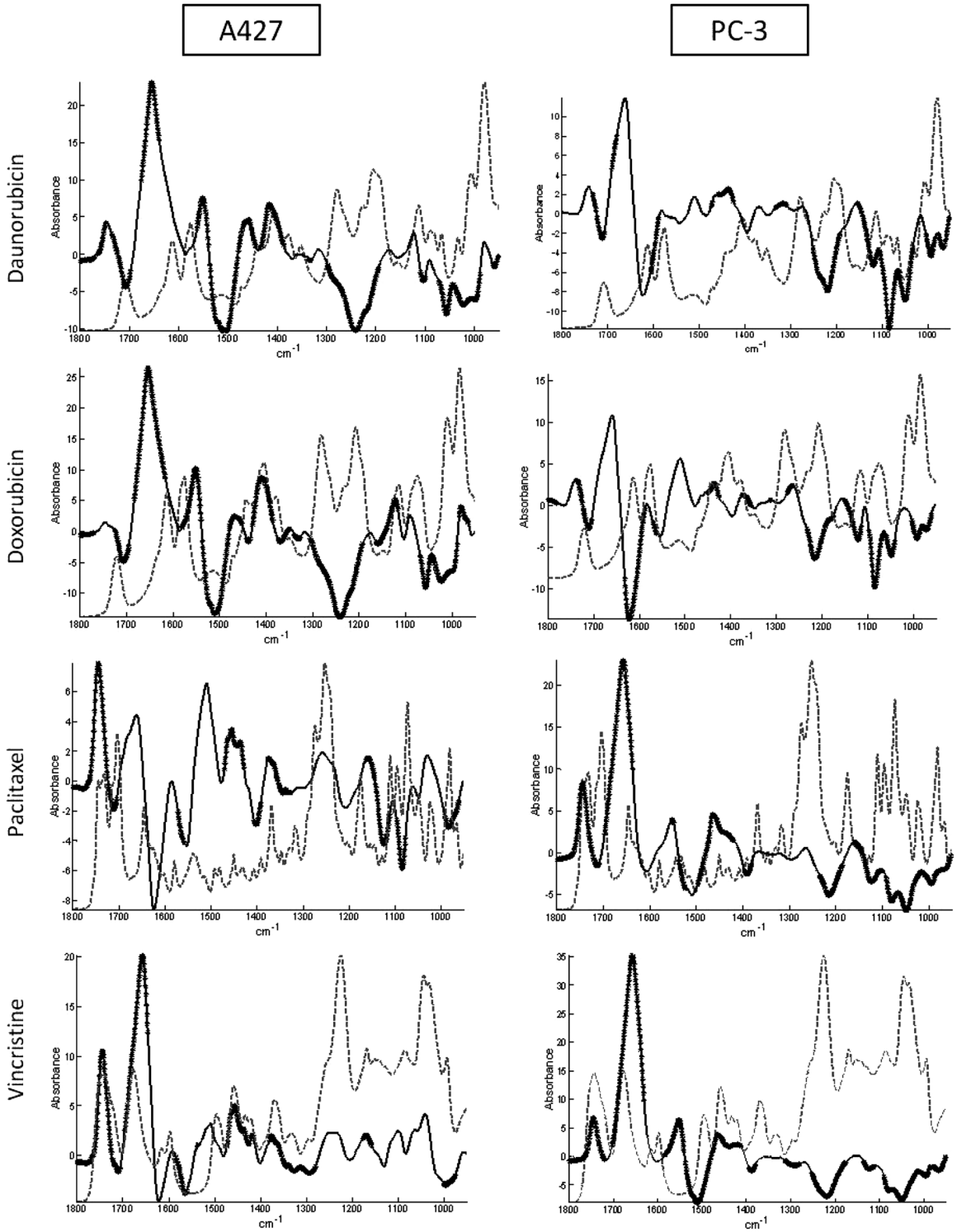

Fig. 7 Comparison between each drug spectrum (dotted line) and the difference spectra of A427 (left) and PC-3 (right) exposed to this drug (indicated on the left). Spectra were superimposed (no offset) and scaled each to fill the window.

characteristics. The purpose of this work was rather to evidence a spectral signature associated with the documented drug mechanism for several drugs on several cell lines.

There is an increasing demand for systemic approaches to study potential drugs and to detect lead compounds. Infrared spectroscopy offers a good opportunity to measure global information on drug "mode of action". Infrared spectra of cells contain information on the genome, proteome, lipidome and metabolome simultaneously. High throughput systems with 96-well plates or more are now available and a well established bioassay could be developed in order to provide an objective classifier for potential anticancer drugs.

Appendix: drug contribution to difference spectra

All drugs were obtained from Sigma (Bornem, Belgium) as powders. The powders were diluted at a concentration of 10^{-3} M in DMSO to insure complete solubility. For cell culture, the drug stock in DMSO was further diluted in culture medium. To assess if drugs could be responsible for the spectral changes, the stock in DMSO was diluted 10 times in water. The infrared spectra of each drug at 10^{-4} M were then recorded. In Fig. 6, spectra of the drugs at 10^{-4} M and the difference spectra corresponding to A427 and PC-3 exposed to daunorubicin are drawn at the same scale. This difference spectrum was obtained with normalized spectra which are approximately multiplied by 1000. In order to provide a correct comparison, drug spectra were also multiplied by 1000. As observed in Fig. 6, at this concentration drugs do not contribute to the IR spectra. Only traces of water vapour are apparent. It must be noticed that 10^{-4} M is a concentration much higher than the concentration used with cells. Indeed, the highest IC_{50} is 1.6×10^{-6} M. Even if 100 fold accumulation occurred in cells, drug molecules could not be responsible for the observed spectral variation.

Another evidence can be provided by the actual infrared spectra of these drugs. 0.5 µl of concentrated drug diluted in water or ethanol was dried on the diamond crystal. Each spectrum was compared with difference spectra of two cell lines (A427 and PC-3) exposed to these drugs. The pure drug spectra and the difference spectra obtained on cells have been superimposed in Fig. 7. Very few similarities can be observed between drug spectra and difference spectra. It confirms that spectral variations observed in this work reflect cellular changes due to exposure to drugs.

Abbreviations

IR	Infrared;
FTIR	Fourier transform infrared;
S/*N*	Signal to noise;
ESS	Error sum of square;
h	Hours.

Acknowledgements

This research has been supported by grants from the National Fund for Scientific Research (FRFC 2.4526.11 and 2.4533.10). E.G. is Director of Research with the "National Fund for Scientific Research" (Belgium), A.D. is Research Fellow supported by the "National Fund for Scientific Research" (Belgium), M.V. is Research Fellow supported by the "F.R.I.A." (Belgium).

References

1 N. D. Yuliana, A. Khatib, Y. H. Choi and R. Verpoorte, *Phytother. Res.*, 2011, **25**, 157–169.
2 S. Rochfort, *J. Nat. Prod.*, 2005, **68**, 1813–1820.
3 H. K. Kim, E. G. Wilson, Y. H. Choi and R. Verpoorte, *Planta Med.*, 2010, **76**, 1094–1102.
4 S. Boydston-white, T. Gopen, S. Houser, J. Bargonetti and M. Diem, *Biospectroscopy*, 1999, **5**, 219–227.
5 E. Goormaghtigh, V. Cabiaux and J. M. Ruysschaert, *Subcell. Biochem.*, 1994, **23**, 405–450.
6 D. Helm, H. Labischinki, G. Schallen and D. Naumann, *J. Gen. Microbiol.*, 1991, **137**, 69–79.
7 D. Naumann, D. Helm and H. Labischinski, *Nature*, 1991, **351**, 81–82.
8 H. Mietke, W. Beer, J. Schleif, G. Schabert and R. Reissbrodt, *Int. J. Food Microbiol.*, 2010, **140**, 57–60.
9 M. A. Cohenford, J. C. Urbanowski and B. Rigas, *Proc. Natl. Acad. Sci. U. S. A.*, 1998, **95**, 15327–15332.
10 B. R. Wood, M. A. Quinn, B. Tait, M. Ashdown, T. Hislop, M. Romeo and D. McNaughton, *Biospectroscopy*, 1998, **4**, 75–91.
11 A. Gaigneaux, C. Decaestecker, I. Camby, T. Mijatovic, R. Kiss, J. M. Ruysschaert and E. Goormaghtigh, *Exp. Cell Res.*, 2004, **297**, 294–301.
12 R. Gasper, T. Mijatovic, A. Bénard, A. Derenne, R. Kiss and E. Goormaghtigh, *Biochim. Biophys. Acta*, 2010, **1802**, 1087–1094.
13 F. Draux, P. Jeannesson, C. Gobinet, J. Sule-Suso, J. Pijanka, C. Sandt, P. Dumas, M. Manfait and G. Sockalingum, *Anal. Bioanal. Chem.*, 2009, **395**, 2293–2301.
14 K. R. Flower, I. Khalifa, P. Bassan, D. Démoulin, E. Jackson, N. P. Lockyer, A. T. McGown, P. Miles, L. Vaccari and P. Gardner, *Analyst*, 2010, **136**, 498–507.
15 A. Derenne, R. Gasper and E. Goormaghtigh, *Analyst*, 2011, **136**, 1134–1141.
16 P. G. Morris and M. N. Fornier, *Clin. Cancer Res.*, 2008, **14**, 7167–7172.
17 V. Srivastava, A. S. Negi, J. K. Kumar, M. M. Gupta and S. P. S. Khanuja, *Bioorg. Med. Chem.*, 2005, **13**, 5892–5908.
18 I. Brown, J. N. Sangrithi-Wallace and A. C. Schofield, in *Anticancer Therapeutics*, ed. S. Missailidis, John Wiley., 2008, pp. 79–90.
19 M. L. Tan, P. F. M. Choong and C. R. Dass, *J. Pharm. Pharmacol.*, 2009, **61**, 131–142.
20 M. M. Paz, in *Anticancer Therapeutics*, ed. S. Missailidis, John Wiley, 2008, pp. 111–132.
21 T. Mosmann, *J. Immunol. Methods*, 1983, **65**, 55–63.
22 M. C. Alley, D. A. Scudiero, A. Monks, M. L. Hursey, M. J. Czerwinski, D. L. Fine, B. J. Abbott, J. G. Mayo, R. H. Shoemaker and M. R. Boyd, *Cancer Res.*, 1988, **48**, 589–601.
23 E. Goormaghtigh, V. Raussens and J. M. Ruysschaert, *Biochim. Biophys. Acta*, 1999, **1422**, 105–185.
24 E. Goormaghtigh, in *Adv. Biomed. Spectrosc*, ed. A. Barth and P. I. Haris, 2009, vol. 2, pp. 104–128.
25 E. Goormaghtigh and J. Ruysschaert, *Spectrochim. Acta*, 1994, **50**, 2137–2144.
26 R. A. Johnson and D. W. Wichern, in *Applied Multivariate Statistical Analysis*, Prentice Hall, Upper Saddle River, 4th edn, 1998, pp. 726–799.
27 J. Joe and H. Ward, *J. Am. Stat. Assoc.*, 1963, **58**, 236–244.
28 R. Gasper and E. Goormaghtigh, *Analyst*, 2010, **135**, 3048–3051.
29 M. Hilvo, C. Denkert, L. Lehtinen, B. Müller, S. Brockmöller, T. Seppänen-Laakso, J. Budczies, E. Bucher, L. Yetukuri, S. Castillo, E. Berg, H. Nygren, M. Sysi-Aho, J. L. Griffin, O. Fiehn, S. Loibl, C. Richter-Ehrenstein, C. Radke, T. Hyötyläinen, O. Kallioniemi, K. Iljin and M. Oresic, *Cancer Res.*, 2011, **71**, 3236–3245.
30 D. Naumann, *Encyclopedia of Analytical Chemistry*, 2000, pp. 102–131.
31 P. Lasch, A. Pacifico and M. Diem, *Biospectroscopy*, 2002, 335–338.
32 M. Diem, S. Boydston-white and L. Chiriboga, *Appl. Spectrosc.*, 1999, **53**, 148A–161A.
33 G. Berger, R. Gasper, D. Lamoral-Theys, A. Wellner, M. Gelbcke, R. Gust, J. Nève, R. Kiss, E. Goormaghtigh and F. Dufrasne, *Int. J. Oncol.*, 2010, **37**, 679–686.
34 R. Gasper, J. Dewelle, R. Kiss, T. Mijatovic and E. Goormaghtigh, *Biochim. Biophys. Acta*, 2009, **1788**, 1263–1270.
35 P. Lasch, M. Boese, A. Pacifico and M. Diem, *Vib. Spectrosc.*, 2002, **28**, 147–157.
36 M. Jackson and H. H. Mantsch, *J. Mol. Struct.*, 1997, **409**, 105–111.
37 T. Abe, S. Hasegawa, K. Taniguchi, A. Yokomizo, T. Kuwano, M. Ono, T. Mori, S. Hori, K. Kohno and M. Kuwano, *Int. J. Cancer*, 1994, **58**, 860–864.
38 L. Rieger, J. Rieger, S. Winter, J. Streffer, P. Esser, J. Dichgans, R. Meyermann and M. Weller, *Acta Neuropathol.*, 2000, **99**, 555–562.
39 L. Ingrassia, F. Lefranc, J. Dewelle, L. Pottier, V. Mathieu, S. Spiegl-Kreinecker, S. Sauvage, M. El Yazidi, M. Dehoux, W. Berger, E. Van Quaquebeke and R. Kiss, *J. Med. Chem.*, 2009, **52**, 1100–1114.
40 T. Mijatovic, U. Jungwirth, P. Heffeter, M. A. R. Hoda, R. Dornetshuber, R. Kiss and W. Berger, *Cancer Lett.*, 2009, **282**, 30–34.
41 H. Nawaz, F. Bonnier, P. Knief, O. Howe, F. Lyng, A. Meadeab and H. Byrne, *Analyst*, 2010, **135**, 3070–3076.